

**COMPARISON OF COASTAL CURRENTS
FROM HF RADAR AND ADCP DATA IN
LEG II**

19 SEPTEMBER 2003

**LCDR Kyung Cheol Kim, ROKN
OC 3570
Summer 2003**

1. INTRODUCTION

There was a research cruise onboard R/V Pt Sur for a group of NPS students studying operational oceanography, OC3570, from 21 to 28 July 2003. Many different types of atmospheric and oceanographic data were collected from numerous locations in the Monterey bay and coastal area between Monterey and San Luis. This report focuses on the analysis of time series data that was collected at the head of the Monterey Canyon from 0300 July 26 to 0600 July 28 GMT and the CODAR-Type HF Radar data operating at Naval Post Graduate School in Monterey, California at the same period.

2. PURPOSE

The origins of HF radar for ocean wave and current measurements began with collaborative work at Stanford University and Scripps Institute of oceanography in the late 1960's. Initial studies focused on wave measurements and the development of a closed-form relation between the radar cross-section and the ocean wave height spectrum.

Results of the 1997 COPE-3 experiment at Chesapeake Bay, Virginia show good statistical comparison between Multi frequency coastal HF radar (MCR) and ADCP measurements of near surface currents (Teague et al., 2001). Based upon this comparison, Teague et al. suggest that the effective depths of the MCR current measurements are consistent with the linear current profile model suggested by Stewart and Joy (1974). In addition, the MCR surface currents, particularly at higher frequencies were well correlated with wind speed, suggesting the utility of this system for mapping the surface wind field.

CODAR-Type HF radar is used to measure the surface currents of the coastal ocean. A transmitter sends out a radio frequency that bounces off the ocean surface and back to a receiver antenna. Using this information and the

principles of the Doppler shift, CODAR is able to calculate the speed and direction of the surface current. These calculations are made at about every half mile across the surface and extend as far as about twenty miles offshore. Using this system, CODAR can calculate surface currents with an error of less than 4 cm/s.

The purpose of this report is to compare the current velocity measured by an Acoustic Doppler Current Profiler (ADCP) at 15 m, 23 m and 31 m depth and by CODAR-Type HF Radar system at the surface of the littoral ocean. This data will also be compared to the wind velocity measured by M1 buoy and the tide data. In addition, the surface current circulation in the Monterey bay will be addressed.

3. DATA COLLECTION

Data collected on two stations off Moss Landing at the head of the Monterey canyon from 0300 July 26 to 0600 July 28 GMT. Figure 3.1 shows the locations of sites used to measure data during the cruise in Monterey bay.

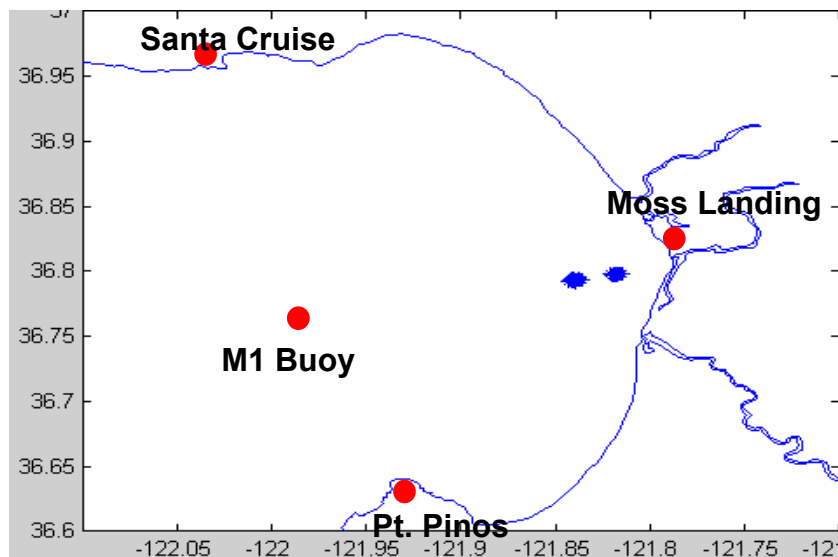


Figure 3.1 – The locations of sites of CODAR-Type HF radar and M1 buoy. Blue dots indicate positions from which ADCP data were collected by R/V Point Sur.

a. ADCP data

The ADCP have transmitter and receiver in one unit and use reflection of the sound wave from drifting particles for the measurement of the Doppler frequency shift. The sound reflects off particles suspended in the water. These particles can be considered to be moving at the same speed as the water and hence, the ADCP ultimately measures the water velocity. Figure 3.2 shows the positions from which ADCP data were collected. All data from the ADCP accepted due to the reasonably scattered positions as expected.

b. CODAR-Type HF Radar

CODAR-Type HF Radar has been employed around Monterey bay, CA, to measure ocean surface currents since February 1992. These instruments located at sites near Monterey and Pt. Pinos in the south and Moss Landing, halfway around the bay to the north and near Santa Cruz on the northern shore of Monterey bay. During the cruise period the site of Monterey was shut down due to a technical problem. And the ocean surface currents are the results of combination measurements of Pt. Pinos, Moss Landing and Santa Cruz site.

c. M1 buoy.

The M-1 buoy is an instrumented mooring maintained by MBARI in Monterey Bay. It is located at 36.775°N , 122.025°W . The buoy was established as part of a network designed to provide continuous in-situ observations of physical, chemical and biological properties over long periods of time. Only wind data from M1 buoy was used for this paper due to the distance from the ADCP stations.

d. Tide

National Oceanic and Atmospheric Administration (NOAA) provides the tide information of Monterey bay area through their subroutine website.

Data collected from ADCP and CODAR-Type HF radar was used to create plots of the currents at each depth. And data collected from M1 buoy and Tide web site of

NOAA was used to give the environmental condition. Figure 3.2 shows the positions from which ADCP data were collected.

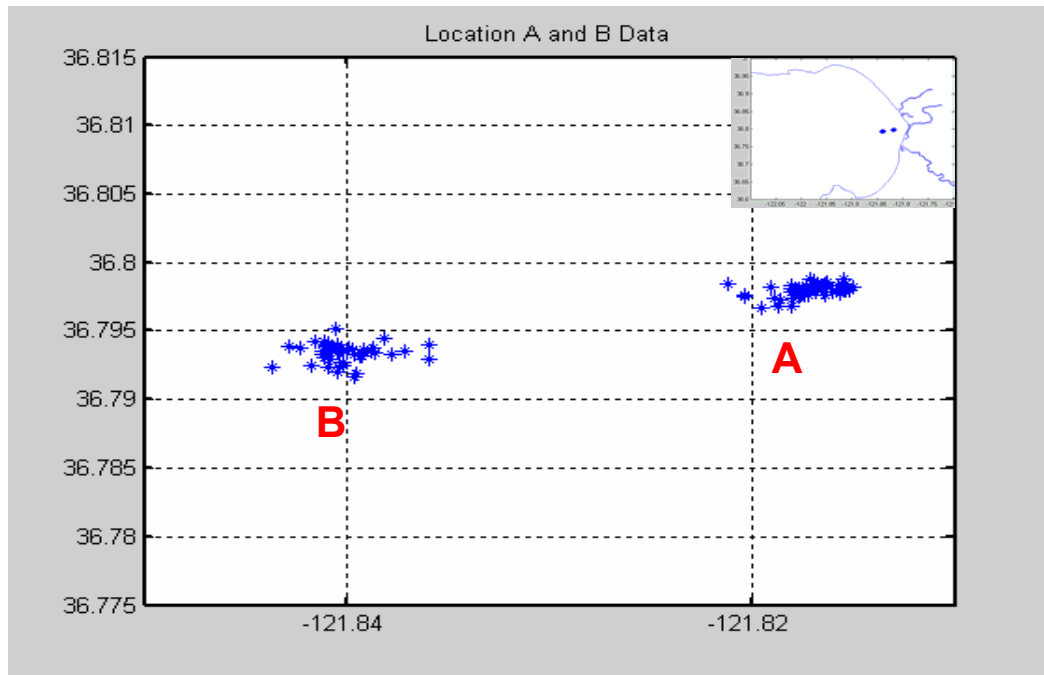


Figure 3.2 – the positions from which ADCP data were collected.

		Total Data	Missing Data	Mean	STD	Time Gap
CODAR HF RD	U At SFC	52	9	-0.57	9.68	60 min
	V At SFC			-0.56	9.5	
ADCP	U At 15m	104	0	0.57 cm/s	4.62	30 min
	U At 23m			1.22 cm/s	5.08	
	U At 31m			2.14 cm/s	4.81	
	V At 15m	104	0	1.56 cm/s	6.78	30 min
	V At 23m			2.41 cm/s	5.61	
	V At 31m			2.91 cm/s	4.36	

Table 4.1 – Summary of CODAR-Type HF radar and ADCP data files

4. DATA ANALYSIS AND INTERPRETATION

Figure 4.1 shows the winds vector as measured by M1 buoy, tides collected from web site and the surface currents as measured by CODAR-Type HF radar and ADCP at 15 m, 23m and 31m depth at two different stations, A and B, during same period. Wind fluctuations are dominated by diurnal wind (sea breeze) forcing and all current fluctuations on the figure are dominated by semidiurnal tidal forcing. Since there is no removal of the tidal component, it is hard to compare the effect of sea breeze on currents.

Figure 4.2 shows scatter diagrams of the east and northward currents measured by the CODAR at surface versus the ADCP currents at 15 m, 23 m and 31 m depth at station A and B. The correlation coefficient between CODAR and ADCP eastward current is less than 0.29 and decreases somewhat with increasing depth. The correlation coefficient of northward current is 0.8215 at 23 m depth and 0.677 at 31 m depth that is much higher than eastward current. Note that the slope of the linear least-squares fit to the data is 1.0719 at 23 m depth and little bit lower at other depth. From this figure, it is easy to see that northward currents have much higher correlation coefficient than the westward currents.

Figure 4.3 shows the comparison of scatter diagrams of the east and northward currents at location-A. The correlation coefficient of eastward currents is -0.2037 at 15 m depth and negatively increases to -0.5567 at 31 m depth with increasing depth. The correlation coefficient of northward currents is 0.5853 at 15 m depth and decreases with increasing depth. Note that the slope of the linear least-squares fit to the data of eastward currents is -1.2811 at 31 m depth that indicates the opposite eastward direction flow with the surface current and also has the relatively high correlation coefficient even though it's negative value.

Figure 4.4 shows the comparison of scatter diagrams of the east and northward currents at location B. The correlation coefficient of both east and northward currents is relatively high at most 0.9966.

	U total	V total	U at A	V at A	U at B	V at B
15 m	0.29	0.8163	-0.2073	0.8866	0.5853	0.8351
23 m	0.2298	0.8215	-0.3137	0.8474	0.575	0.9069
31 m	0.0059	0.677	-0.5567	0.6941	0.3816	0.8164

Table 4.2 – Correlation coefficient of east and northward velocity between ADCP and CODAR at 15 m, 23 m and 31 m depth.

Figure 4.5 shows the surface current field of Monterey bay on 26 July 2003 at 0400 GMT with the current of ADCP at 31 m depth and tide status. From this figure, it is easy to see that the direction of surface current is nearly opposite with the current at 31 m depth.

Figure 4.6 shows the surface current field of the bay on 26 July 2003 at 1800 GMT with the current of ADCP at 15 m depth and tide status. There was no tidal forcing at that time and both surface and 15 m depth currents are moving together toward south.

Figure 4.7 shows the surface current field of the bay on 27 July 0400 GMT with the current of ADCP at 31 m depth and tide status. This figure has almost same phenomena with figure 4.5 that has the opposite direction currents at 31 m depth with the surface currents.

Figure 4.8 shows the surface current circulation in Monterey bay from 0300 July 26 to 0400 July 27 and Figure 4.9 shows the surface current circulation in Monterey bay from 0500 July 27 to 0600 July 28. It shows dynamic cyclonic and anticyclonic circulation and eastward movement with time change in Monterey bay. The semidiurnal-period motions due to tidal forcing are clearly shown on the figures. But the effect of wind forcing or currents flowing outside of the bay is not clear.

5. Results and Conclusion

Previous experiments show the efficiency of HF radar to measure the near surface currents. Also CODAR-Type HF radar can calculate surface currents with an error of less than 4 cm/s.

Surface currents around Monterey bay exhibit strong fluctuations with periods in the tidal bands. The semidiurnal-period motions are largely due to forcing by the dominant M2 (12.4 hr) tidal constituent. Diurnal motions, on the other hand, are largely explained by fluctuations of the wind at, approximately, diurnal (~24 hr) periods (Paduan et al., 1997). From analysis of the results presented here, it also clearly shows the semidiurnal-period motions forced by the dominant M2 (12.4 hr) tidal constituent. But it's not clear the diurnal motions on surface currents by CODAR-Type HF radar because there was no removal of the tidal component from CODAR-Type HF radar observations.

Two stations time series shows that most of east and northward currents have high correlation coefficient except eastward currents at station-A. The eastward current at station-A shows the opposite direction flow at 31 m depth with surface currents with relatively high negative correlation coefficient. It is not easy to explain with a couple reasons to explain this process. First there is a topographic reason. It is located very closely to the coast of Moss Landing with 160 m depth at the head of Monterey canyon. There is no space to flow toward east due to this boundary. This affects more on eastward currents than westward currents. The other side station-B located further off the coast with 250 m depth that has less effect of boundary condition and bottom friction. Another possible reason is the effect of wind and tidal forcing. Wind fluctuations are dominated by diurnal wind (sea breeze) that is stronger in eastward direction than northward direction. Further more the difference of measured depth possibly effects this results.

The understanding of coastal oceanic parameters is extremely difficult because winds, waves, and currents interact with the boundaries on much smaller space and time scales than open ocean. Further studies are required with several layers' velocity up to the bottom and longer time series for better understanding this process.

6. REFERENCES

Jeffrey D. Paduan and Hans C. Graber, Introduction to High-frequency Radar: Reality and Myth, 1997

Jeffrey D. Paduan and Michael S. Cook, Mapping Surface Currents in Monterey Bay with CODAR-Type HF Radar, 1997

David Prandle, Tidal and Wind-Driven Currents from OSCAR, 1997

Kristen Watts, The Internal Tidal bore at the Head of the Monterey Submarine Canyon, 1997

Lorell A. Meadows, High Frequency Radar Measurements of Friction Velocity in the Marine Boundary Layer, 2002

<http://marine.rutgers.edu/mrs/codar.html>

<http://tidesonline.noaa.gov/>

http://www.oc.nps.navy.mil/~icon/frames/mooring_frame.html

http://www.oc.nps.navy.mil/~icon/frames/hfradar_frame.html

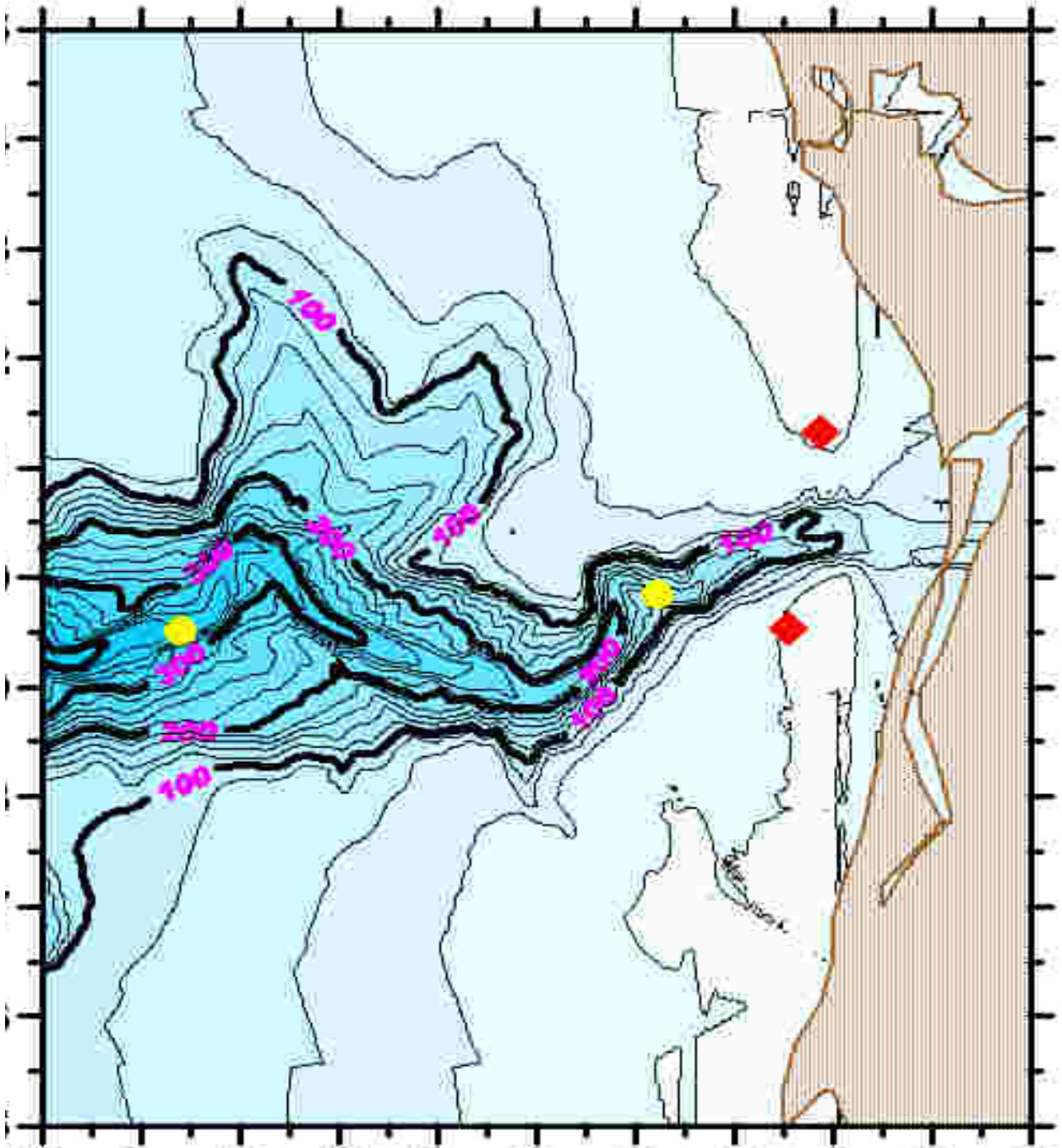


Figure 3.3 – Bathymetry at the head of the Monterey Canyon

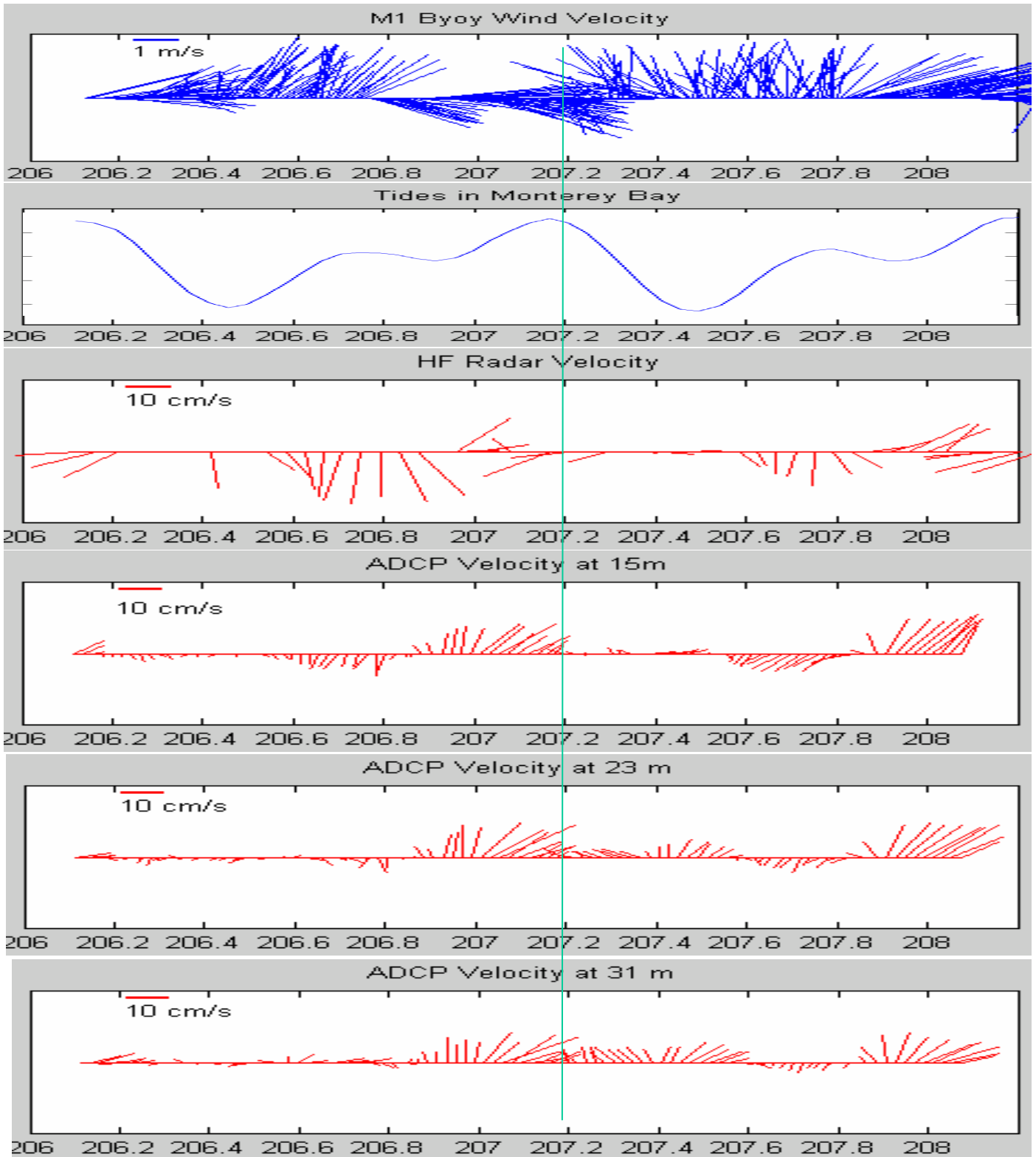


Figure 4.1 – Winds measured by M1 Buoy, Tides, Currents measured by CODAR-Type HF radar and ADCP

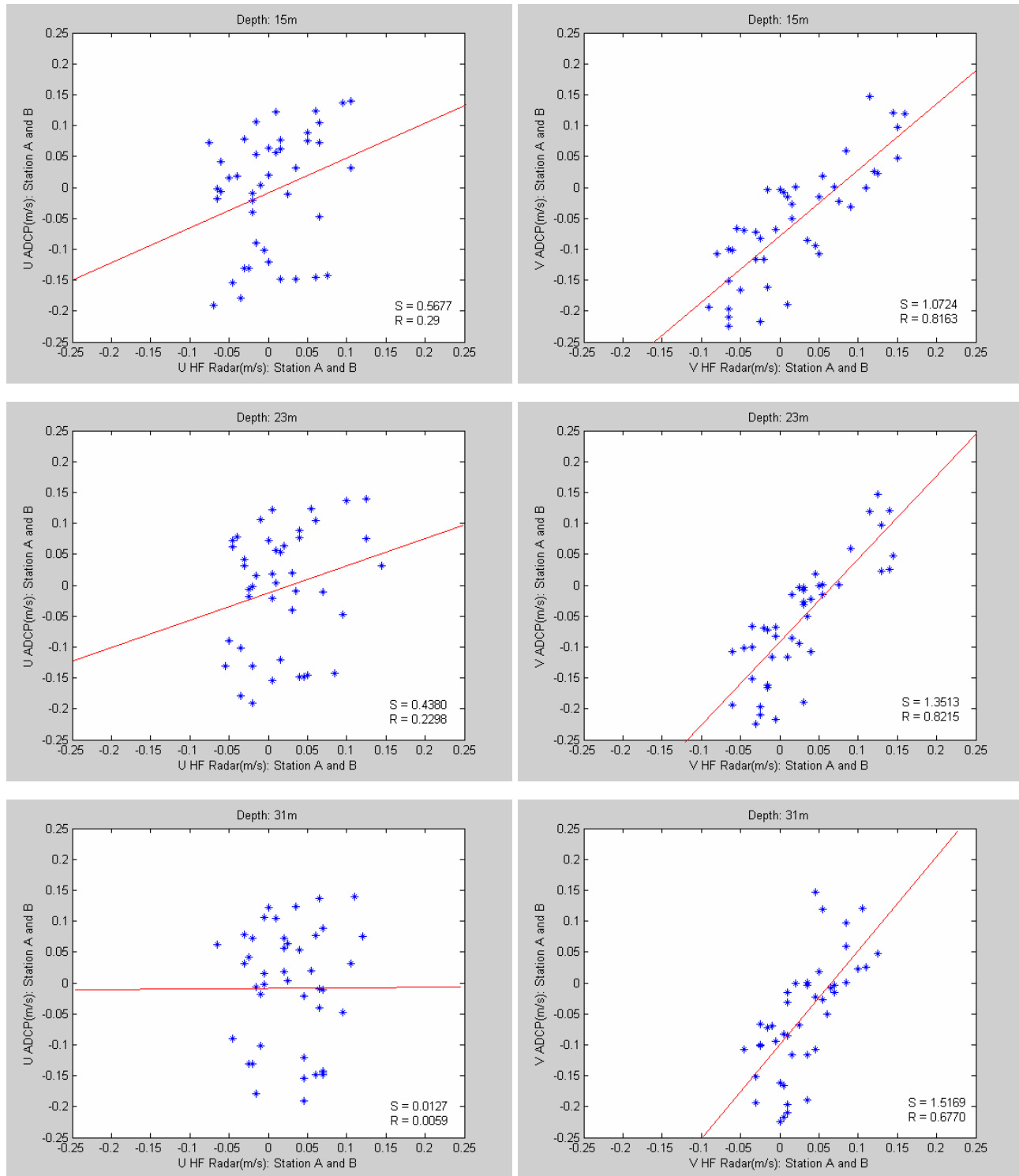


Figure 4.2 - Plots of the eastward and northward CODAR and ADCP currents measured at location A and B. The slope S of the linear fit and the correlation coefficient R between the CODAR and ADCP currents are noted for each depth.

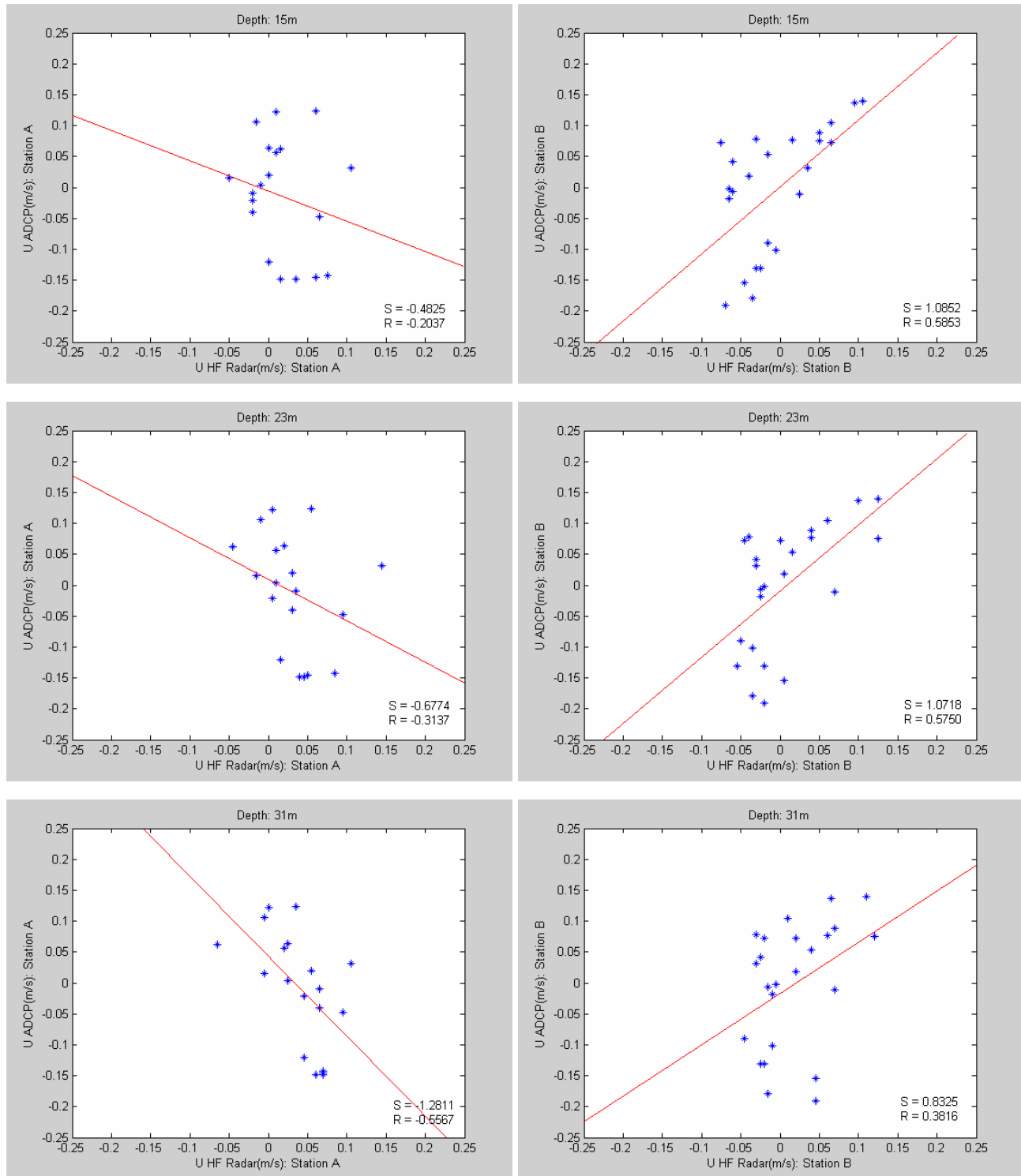


Figure 4.3 - Plots of the eastward CODAR and ADCP currents measured at location A and B. The slope S of the linear fit and the correlation coefficient R between the CODAR and ADCP currents are noted for each depth.

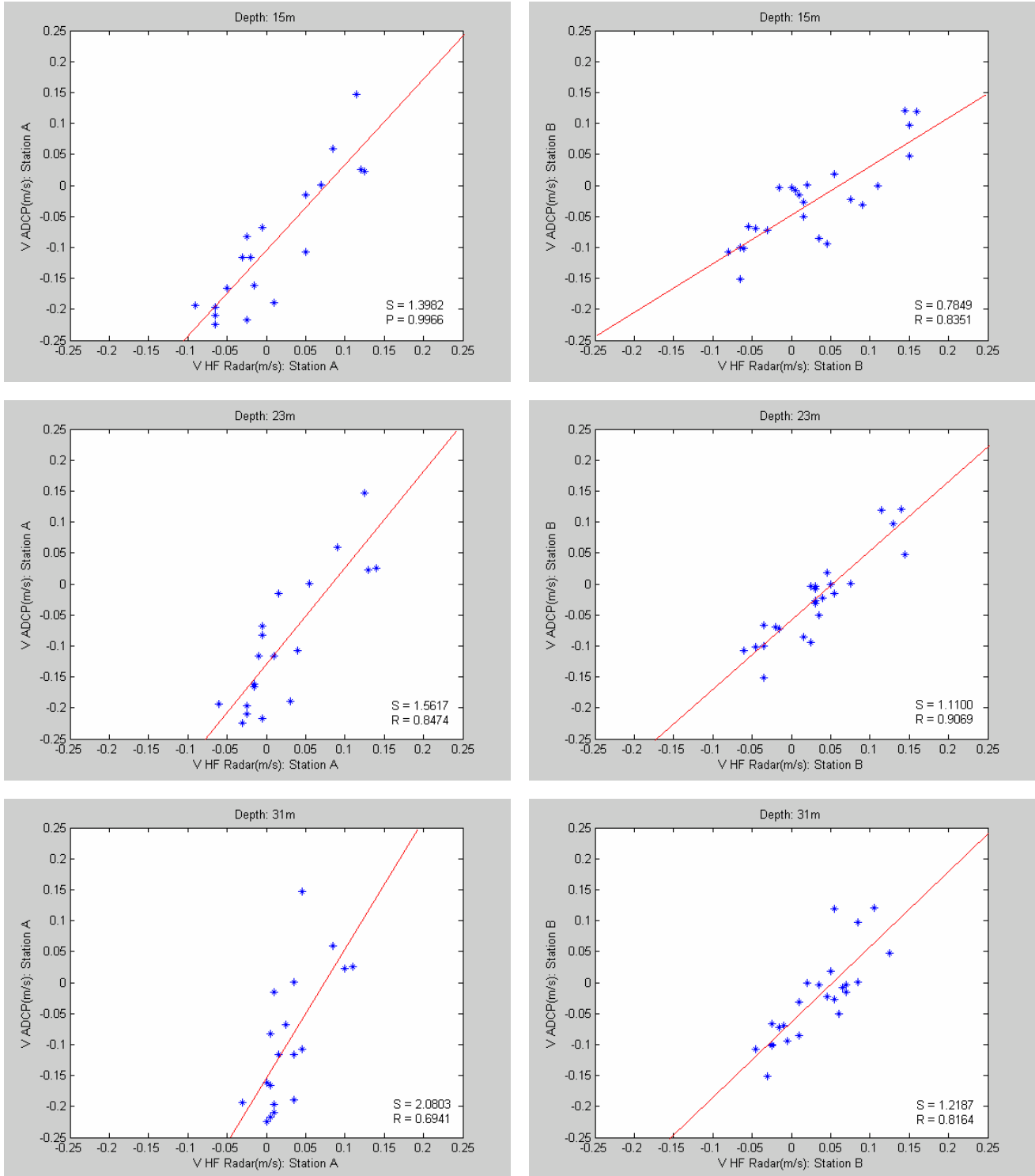


Figure 4.4 - Plots of the northward CODAR and ADCP currents measured at location A and B. The slope S of the linear fit and the correlation coefficient R between the CODAR and ADCP currents are noted for each depth.

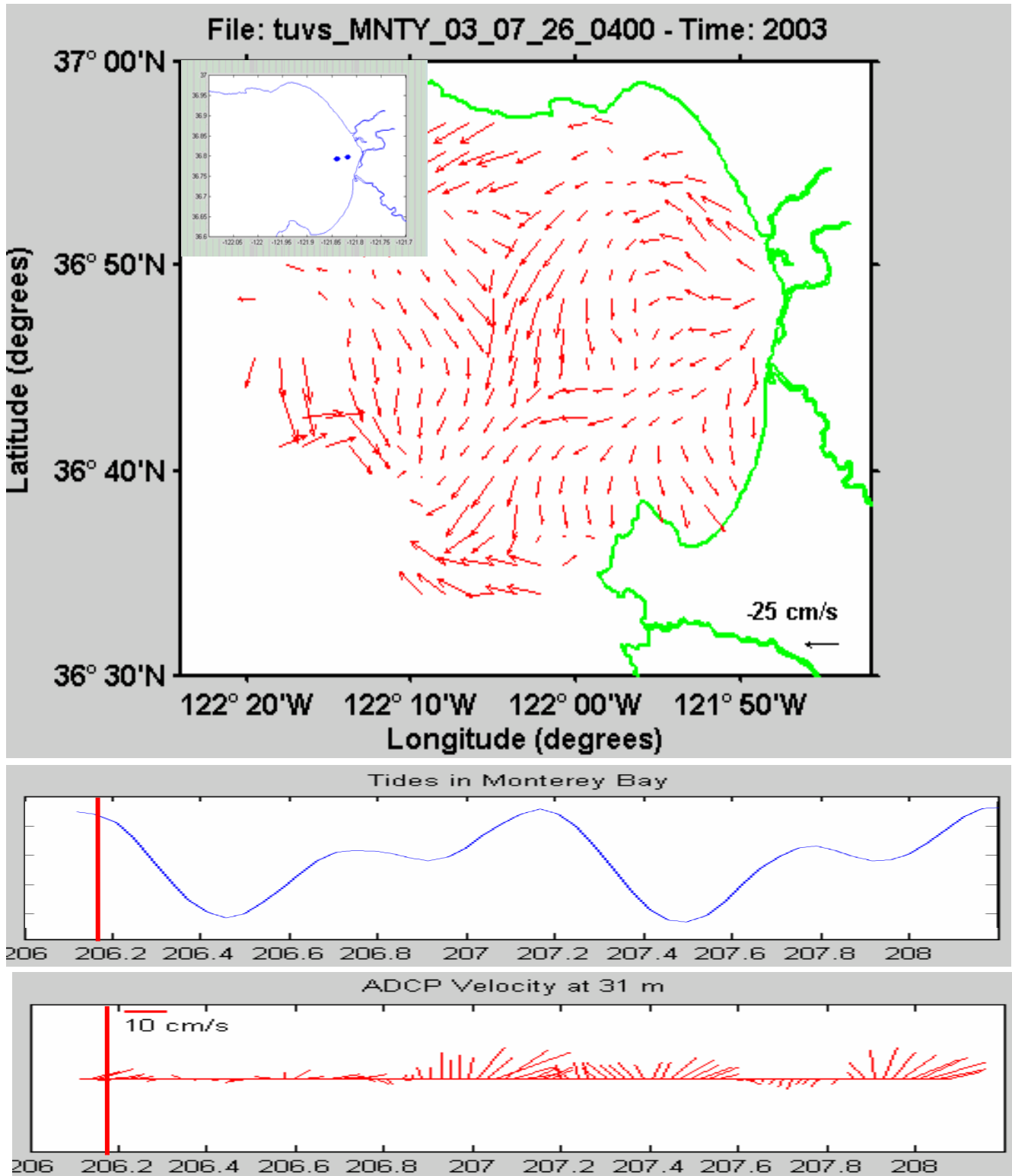


Figure 4.5 - The surface current field of Monterey bay on 26 July 2003 at 0400 GMT with the current of ADCP at 31 m depth and tide status

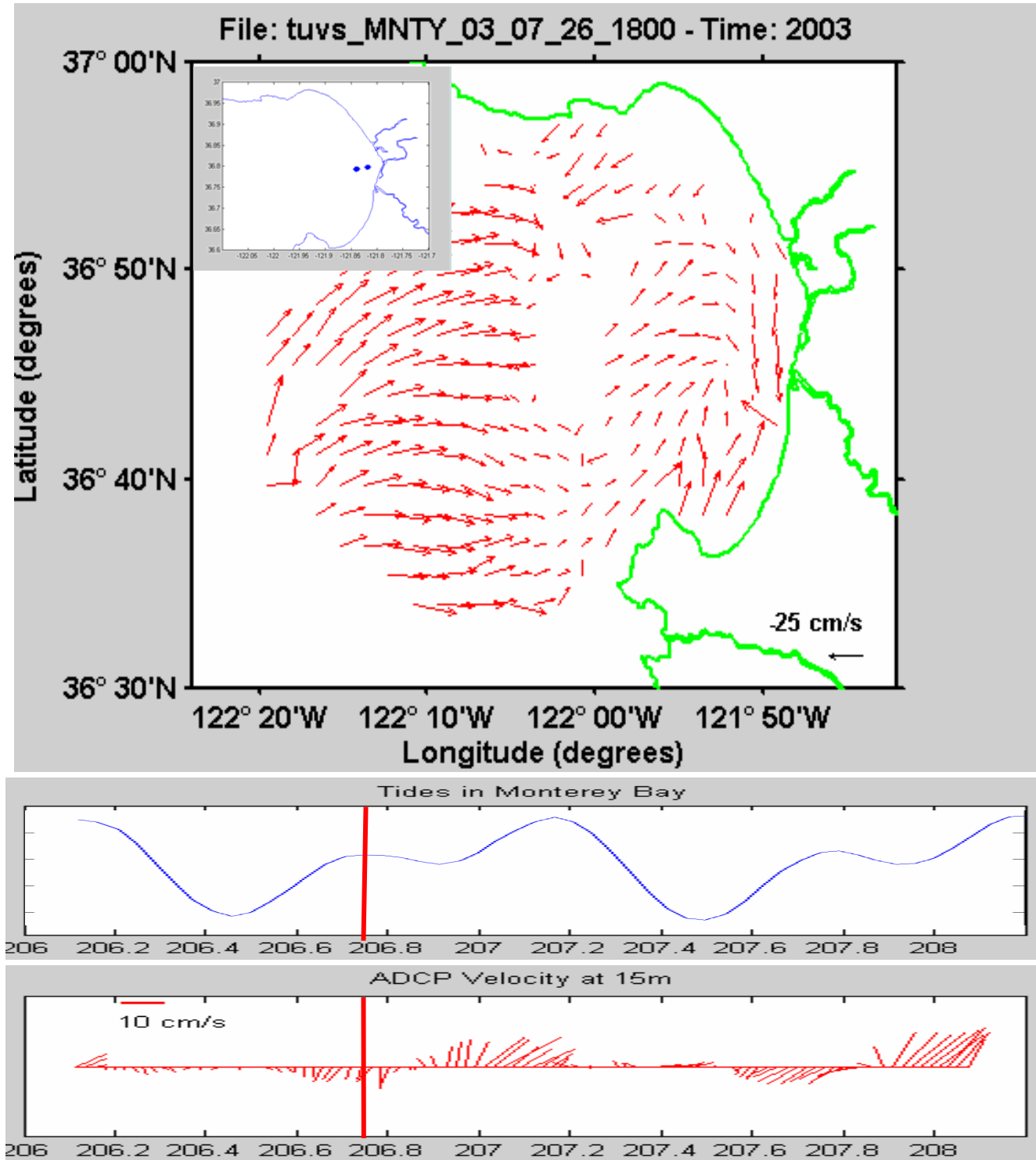


Figure 4.6 - The surface current field of Monterey bay on 26 July 2003 at 1800 GMT with the current of ADCP at 15 m depth and tide status

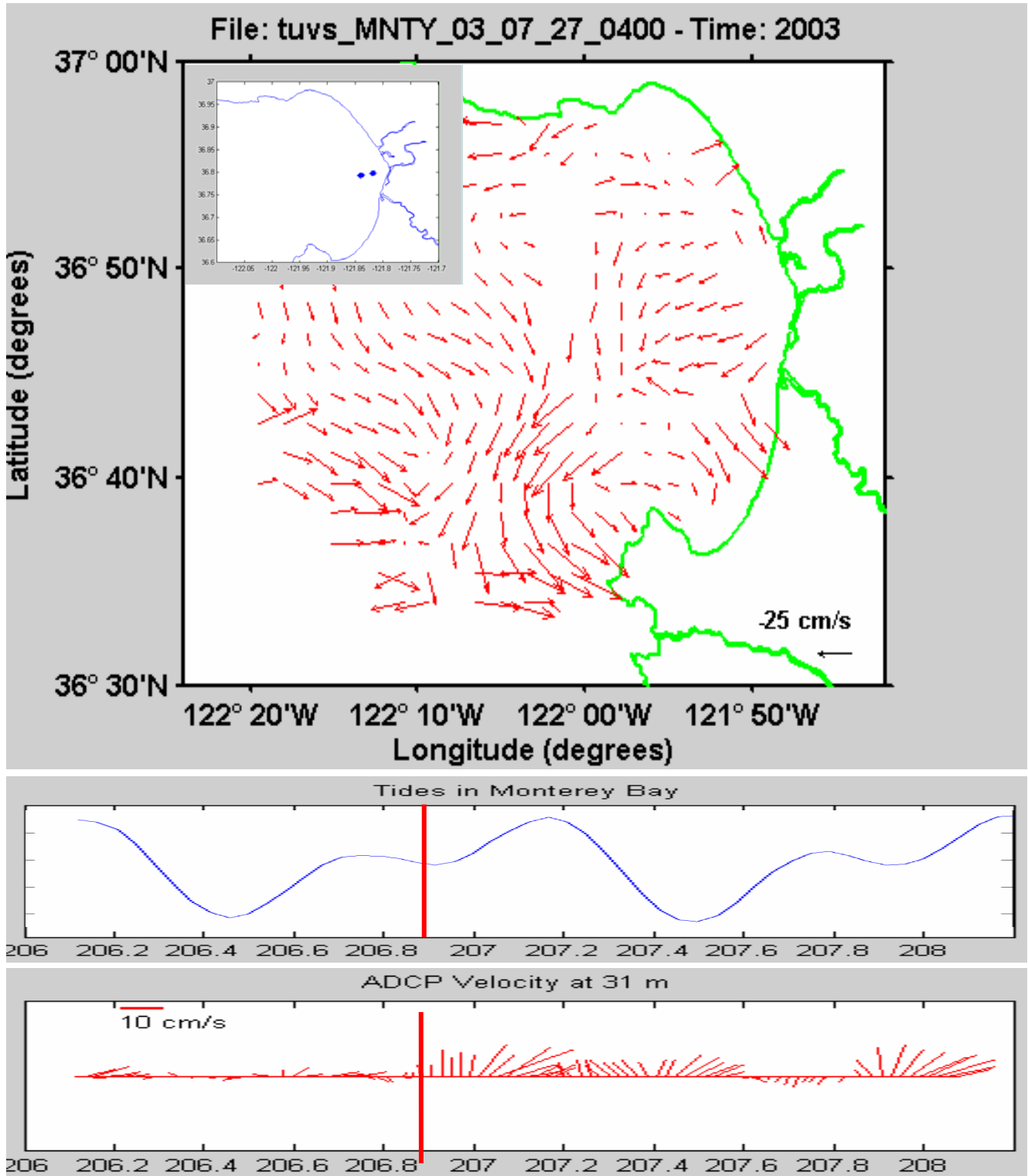
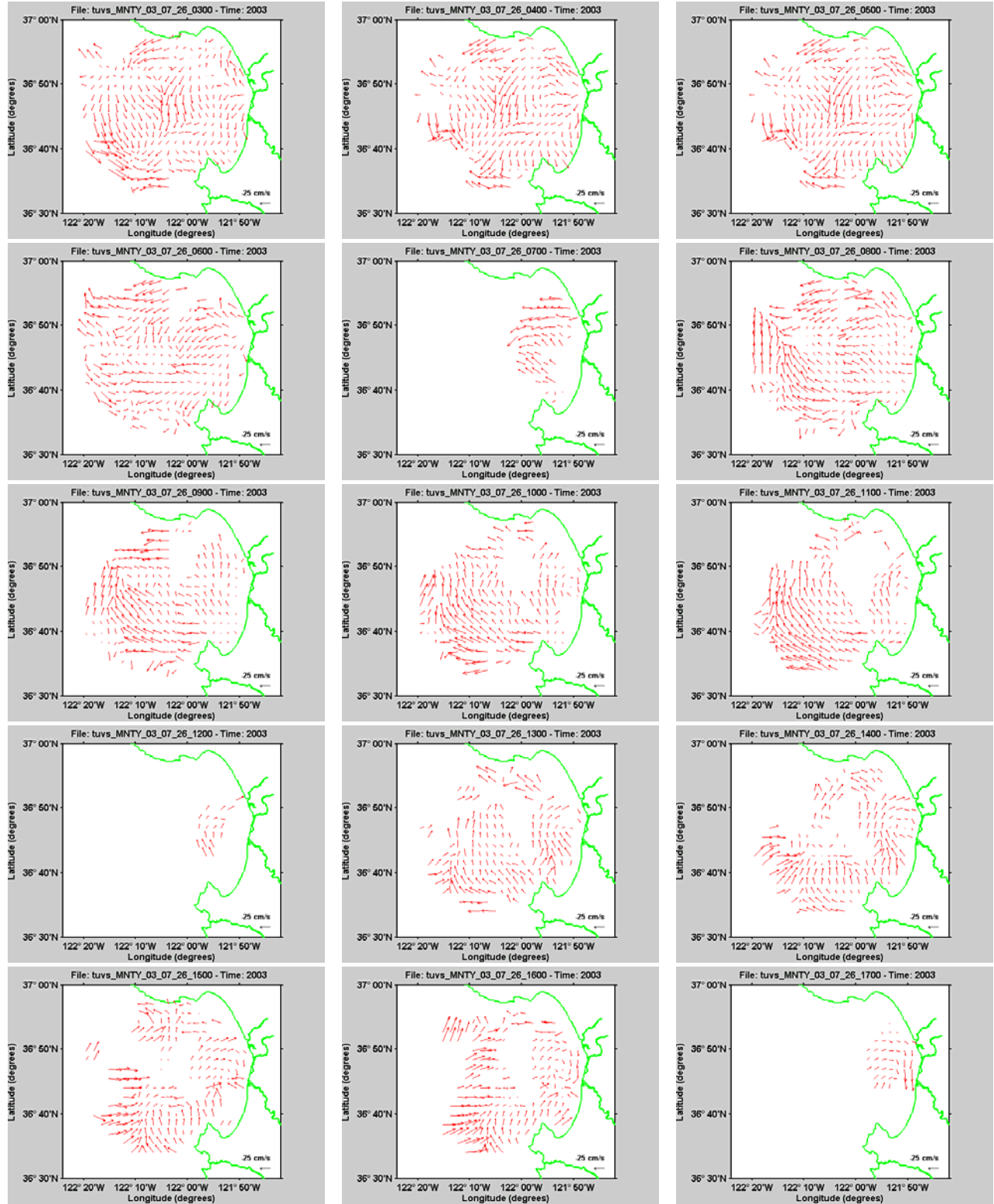


Figure 4.7 - The surface current field of Monterey bay on 27 July 2003 at 0400 GMT with the current of ADCP at 31 m depth and tide status



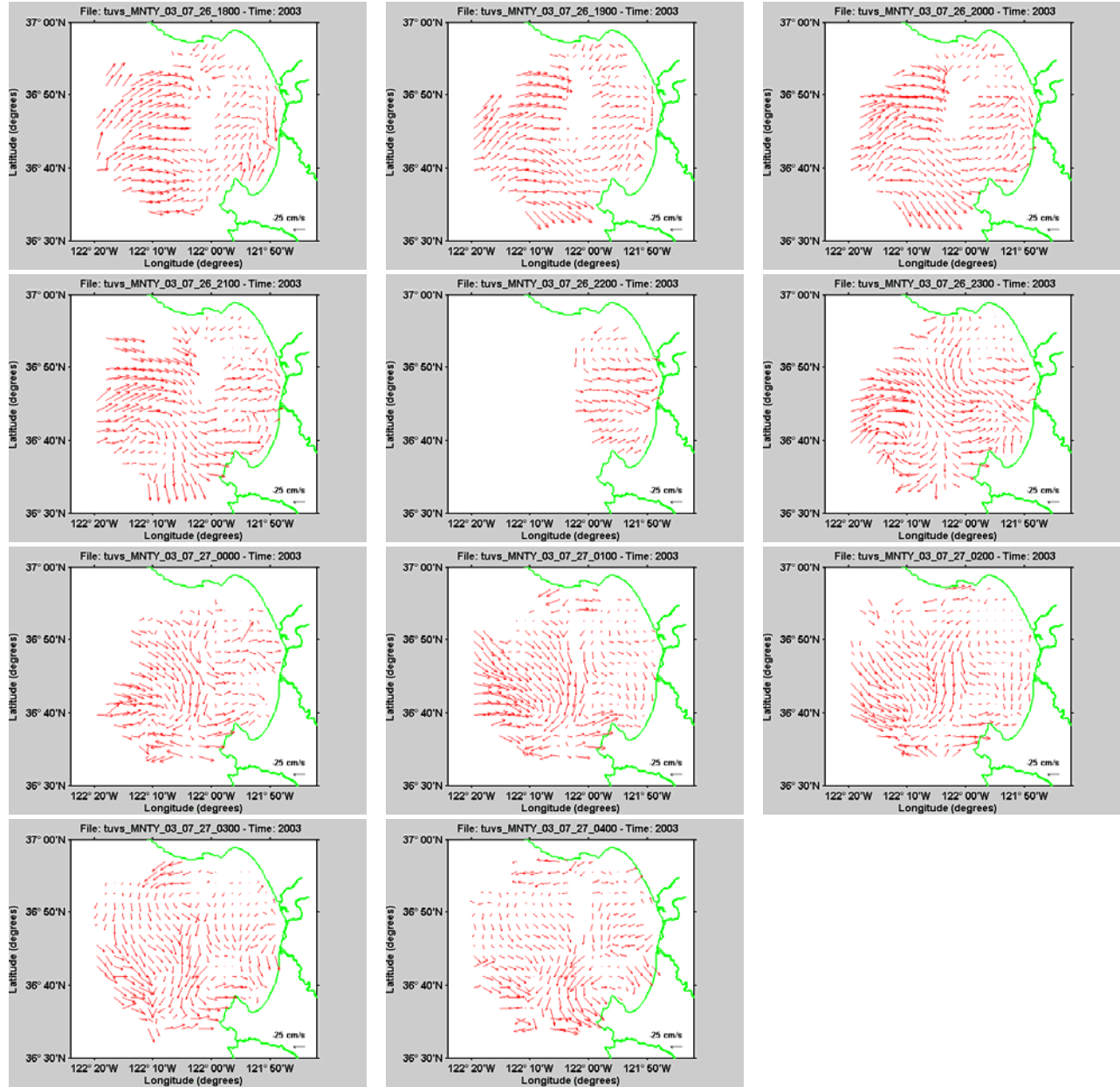
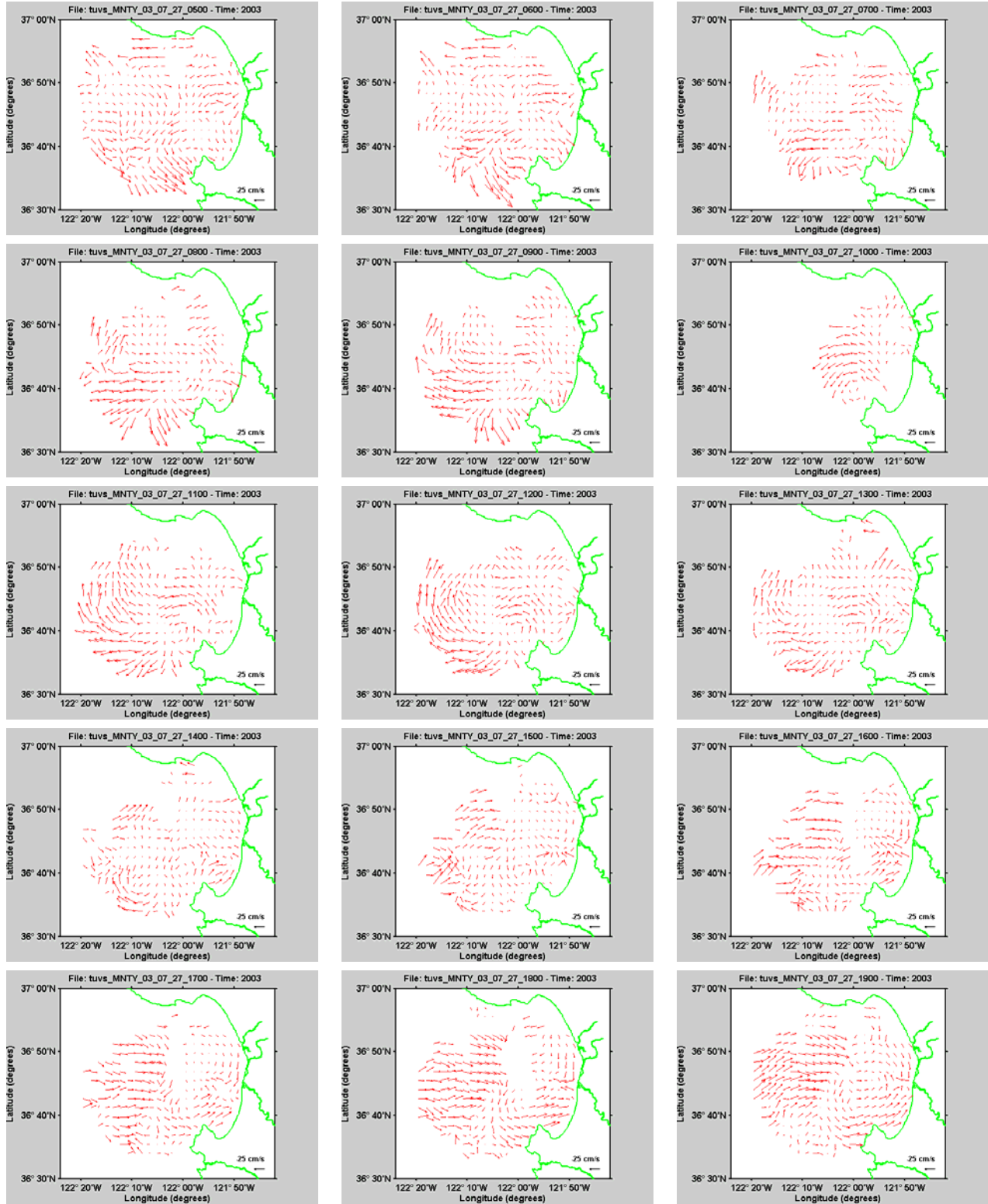


Figure 4.8 - The surface current circulation in Monterey bay from 0300 July 26 to 0400 July 27 GMT



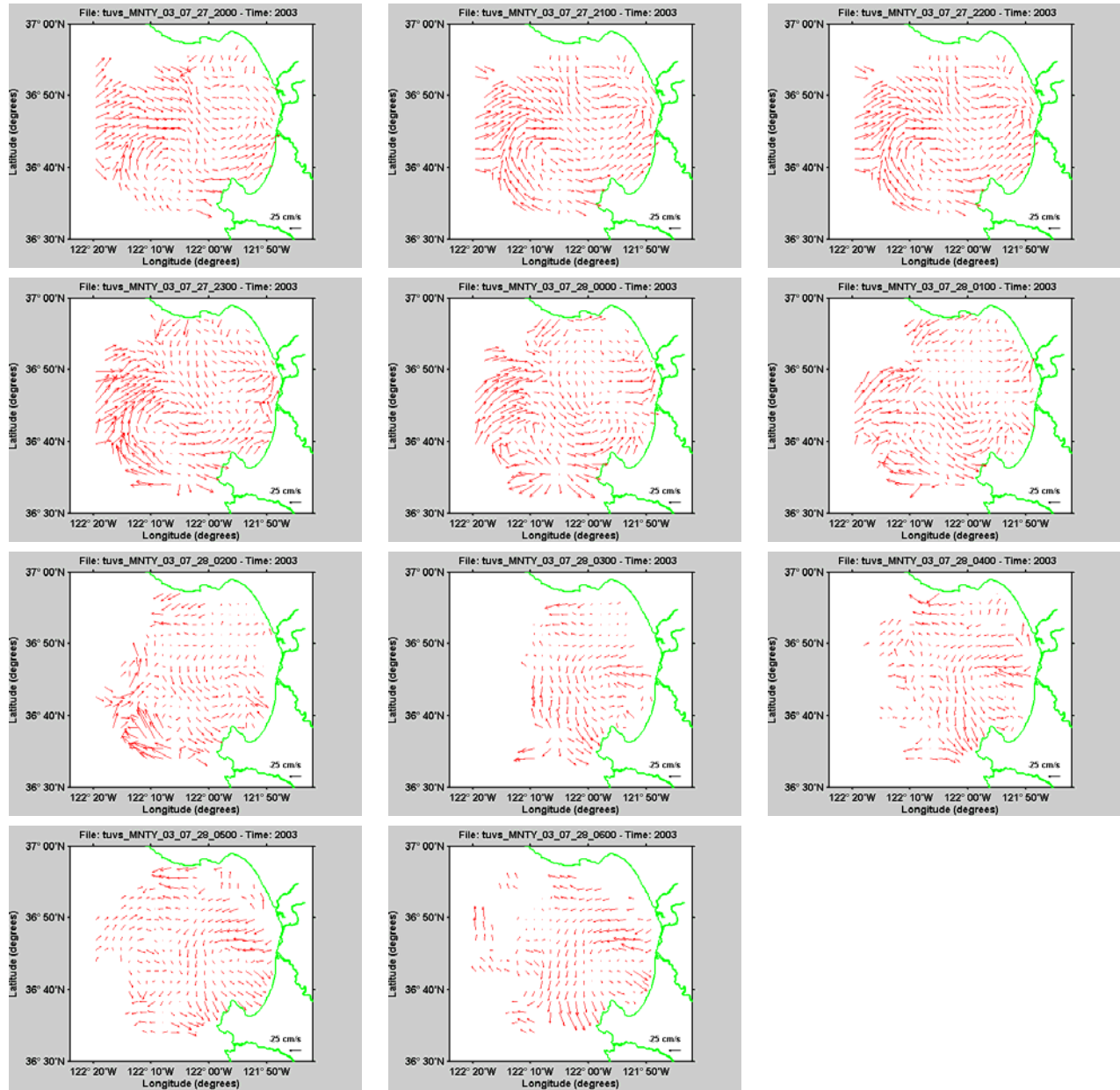


Figure 4.9 - The surface current circulation in Monterey bay from 0500 July 27 to 0600 July 28 GMT